BIOCHEMISTRY
including biophysical chemistry & molecular biology

Article

pubs.acs.org/biochemistry

Hysteresis in Human UDP-Glucose Dehydrogenase Is Due to a Restrained Hexameric Structure That Favors Feedback Inhibition

Renuka Kadirvelraj,[†] Gregory S. Custer,[†] Nicholas D. Keul, Nicholas C. Sennett, Andrew M. Sidlo, Richard M. Walsh, Jr., and Zachary A. Wood*

Department of Biochemistry & Molecular Biology, University of Georgia, Athens, Georgia 30602, United States

ABSTRACT: Human UDP-α-D-glucose-6-dehydrogenase (hUGDH) displays hysteresis because of a slow isomerization from an inactive state (E*) to an active state (E). Here we show that the structure of E* constrains hUGDH in a conformation that favors feedback inhibition at physiological pH. The feedback inhibitor UDP-α-D-xylose (UDP-Xyl) competes with the substrate UDP-α-D-glucose for the active site. Upon binding, UDP-Xyl triggers an allosteric switch that changes the structure and affinity of the intersubunit interface to form a stable but inactive horseshoe-shaped hexamer. Using sedimentation velocity studies and a new crystal structure, we show that E* represents a stable conformational intermediate between the active and feedback-inhibited conformations. Because the allosteric switch occludes the cofactor and substrate binding sites in the inactive hexamer, the intermediate conformation observed in the crystal structure is consistent with the E* transient observed in relaxation studies. Steady-state analysis shows that the E* conformation enhances the affinity of hUGDH for the allosteric inhibitor UDP-Xyl by 8.6-fold (K_i = 810 nM). We present a model in which the constrained quaternary structure permits a small effector molecule to leverage a disproportionately large allosteric response.

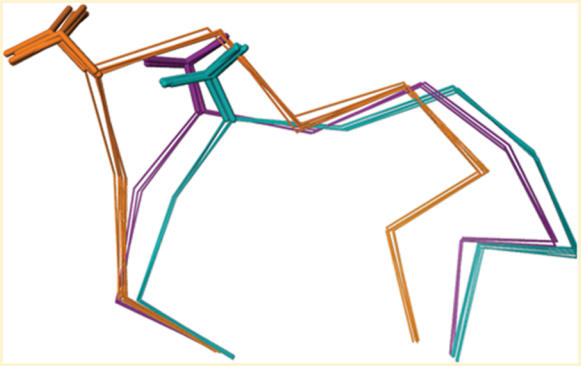

Human UDP-α-D-glucose-6-dehydrogenase (hUGDH) catalyzes the NAD^+-dependent oxidation of UDP-α-D-glucose (UDP-Glc) to produce UDP-α-D-glucuronic acid.[1−4] In solution, apo-hUGDH forms a hexamer built from three weakly interacting dimers.[5−7] Because of the weak affinity between subunits, the apo hexamer easily dissociates at low protein concentrations. We have previously shown that dimer association is under allosteric control.[5,6,8] The feedback inhibitor UDP-α-D-xylose (UDP-Xyl) binds to the active site and triggers an allosteric switch that increases the affinity between the subunit interfaces to form a stable, horseshoe-shaped hexamer (Figure 1A,B).[8] In the horseshoe conformation, the allosteric switch sterically occludes the binding sites for the cofactor and the C5′-hydroxymethyl on the substrate to inactivate the enzyme (Figure 1B). Because the allosteric switch responds to the absence of a C5′-hydroxymethyl in UDP-Xyl, the substrate UDP-Glc has no effect on the affinity between subunits or hexamer formation (Figure 1B).[5,6,8] In contrast, binding of the cofactor (NAD^+) allosterically increases the affinity between subunits and induces the formation of an active, *32 symmetry* hexamer (Figure 1A).[6] hUGDH is unusual in that the allosteric and active sites are present as a single site with distinct induced-fit responses that control subunit affinity and quaternary structure.[8]

In addition to allostery, hUGDH also displays hysteresis, which can be observed as a lag in progress curves (Figure 1C).[7,9] Hysteresis can occur when an enzyme undergoes a slow transition from an inactive conformation (E*) to a more active state (E) in the presence of substrate or an allosteric effector (Figure 1D).[10] We have recently shown that the lag in hUGDH is not due to the association of dimers or the dissociation of the hexamer or another aggregate.[7] Instead, hUGDH hysteresis is due to a cofactor and substrate-induced isomerization of the E* conformation to form the active enzyme (Figure 1D).[7] Previous work[7] has shown that the hysteretic transition in hUGDH is most consistent with the ligand-induced slow transition (LIST) model in which the binding of the cofactor to the binary E*:UDP-Glc complex induces a slow isomerization to the active (or more active) E:UDP-Glc:NAD^+ complex (Figure 1D).[10] Here we show that the E* structure represents a conformational intermediate between the active *32 symmetry* and inactive horseshoe hexamers. Because the only difference between UDP-Xyl and UDP-Glc is the absence of a C5′-hydroxymethyl group in the inhibitor, we argue that the function of the intermediate, E*, is to leverage the conformation of hUGDH into a state that can easily switch to the inhibited complex.

MATERIALS AND METHODS

Protein Expression and Crystallization. Wild-type hUGDH was recombinantly expressed and purified, and the

Received: May 16, 2014
Revised: December 4, 2014
Published: December 5, 2014

   dx.doi.org/10.1021/bi500594x | *Biochemistry* 2014, 53, 8043−8051

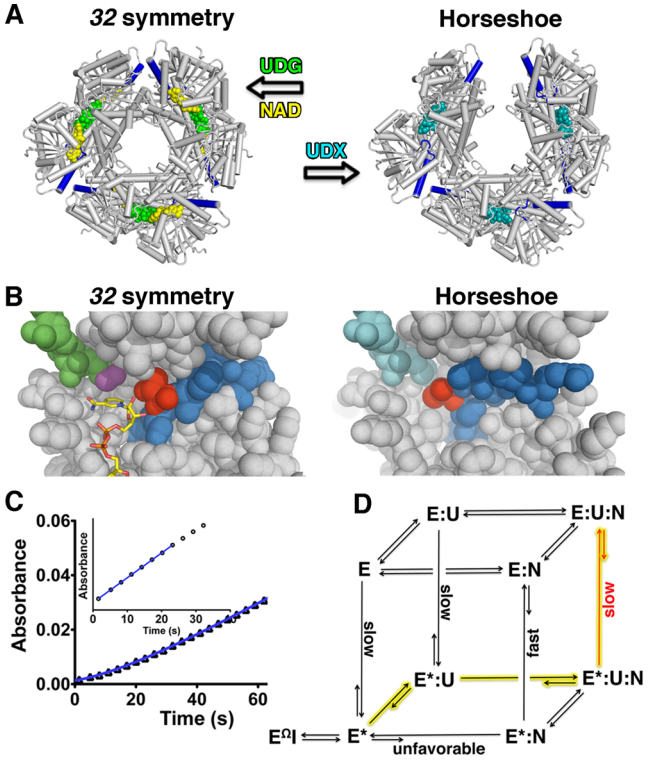

Figure 1. Allostery and hysteresis in hUGDH. (A) hUGDH hexamer depicted in the active, *32 symmetry* and inactive horseshoe-shaped conformations. UDP-Glc (UDG, green), NAD^+ (yellow), and UDP-Xyl (UDX, cyan) are depicted as spheres. Changes in the Thr131 loop (blue loop) conformation will alter the affinity of the subunit interface via the α6 helix (blue rod).[8] For the sake of clarity, only the top trimer of dimers in the hexamer is depicted. (B) Active site showing the Thr131 loop (blue spheres with Thr131 colored red) in the *32 symmetry* and horseshoe conformations. NAD^+ (yellow sticks) buttresses the Thr131 loop to increase the affinity between subunit interfaces and induce formation of the active hexamer.[6] The Thr131 loop switches conformation in response to UDP-Xyl (cyan) binding, to occlude the binding sites for NAD^+ and the C5′-hydroxylmethyl (magenta spheres) of UDP-Glc (green spheres).[8] The inhibited conformation also increases the affinity between dimers to induce formation of the horseshoe hexamer. For the sake of clarity, residues burying the active site and Thr131 loop have been removed. (C) hUGDH progress curves showing that hysteresis is a property of the hexamer and that there is no lag in the dimer (inset). The lag is fit (blue line) with eq 1 from Materials and Methods. This figure is modified from ref 7. (D) Ligand-induced structural transition (LIST) model[10] for hUGDH hysteresis based on our earlier work.[7] Inactive complexes are identified with an asterisk, and E* is the thermodynamically favored conformation of the apoenzyme. Unequal arrows identify favored directions supported by our earlier kinetic studies.[7] The binding of UDP-Glc (U) to E* is $>10^4$-fold faster than the binding of NAD^+ (N) and thus represents the kinetically preferred path of substrate addition (highlighted in yellow).[7] Subsequent binding of cofactor N to form the ternary E*:U:N complex induces a slow isomerization to the active, E:U:N Michaelis complex. This transition is observed as the lag in progress curves. Turnover of the complex produces E, which can rapidly bind substrate and cofactor to form the E:U:N complex or slowly convert to the more stable E* at low substrate concentrations. It is possible that the E*:U:N complex is active, but turnover would necessarily be slow to cause hysteresis. The isomerization of the E*:N complex to the E:N complex is inferred from our previous work showing that binding of U to the saturated E:N complex does not display hysteresis.[7]

Table 1. Data Collection and Refinement Statistics

Data Collection	
space group	C2
unit cell dimensions (*a*, *b*, *c*, *β*)	176.98 Å, 113.96 Å, 97.12 Å, 116.9°
completeness (%)	99.3 (97.4)[a]
no. of reflections	350028
redundancy	7.4 (7.3)
$I/\sigma(I)$	19.6 (1.5)
R_{meas}[b] (%)	12.7 (162.5)
$CC_{1/2}$[c]	0.999 (0.655)
Refinement	
resolution (Å)	2.7
R_{work}/R_{free}[d]	0.18/0.23
no. of atoms	
protein	10830
ligand	4
water	8
B factor (Å^2)	
protein	86.8
ligand	105.7
water	62.7
stereochemical ideality	
bond lengths (Å^2)	0.009
bond angles (deg)	1.1
φ,*ψ* most favored (%)[e]	97.4
φ,*ψ* additionally allowed (%)[e]	2.6

[a]Values in parentheses are for the highest-resolution shell (2.7−2.86 Å). [b]R_{meas} is the redundancy-independent merging *R* factor of Diederichs and Karplus.[30] [c]$CC_{1/2}$ is the correlation between intensities from random half-data sets.[31] [d]An *a posteriori* R_{free} was obtained as explained in Materials and Methods. [e]Values obtained from structure validation using MolProbity.[32]

His tag was removed as described previously.[8] The purified protein was dialyzed into storage buffer [25 mM Tris (pH 8) and 200 mM NaCl] and concentrated to 10 mg/mL. Crystals were grown at 20 °C using the hanging drop vapor diffusion method with 2 μL drops mixed in a 1:1 ratio (protein:reservoir). The reservoir contained 50 mM sodium formate, 15% PEG 3350, and 100 mM HEPES (pH 7.0).

Data Collection, Structure Solution, and Refinement. Crystals were cryoprotected with the reservoir solution containing 21% glycerol, ethylene glycol, and dimethyl sulfoxide in a 1:1:1 ratio and plunged into liquid nitrogen prior to data collection. The 2.7 Å resolution data were collected at the 22-BM beamline (SER-CAT) at the Argonne National Laboratory (Argonne, IL) using a MAR 225 mm CCD detector, a wavelength of 1 Å, and an oscillation step of 1.0° for 360°. Data were processed with XDS,[11] and 8% of the data were set aside for cross-validation. The crystal parameters and data collection statistics are summarized in Table 1.

The structure of E* was determined by molecular replacement using the PHENIX software suite.[12] Molecular replacement was conducted using an unpublished crystal structure of hUGDH lacking the extreme C-terminus (residues 467−494) as the search model. The model was subjected to rigid body and positional refinement using the PHENIX software suite.[12] Refinement consisted of iterative cycles of manual rebuilding using COOT followed by automated refinement with PHENIX.[12,13] The *B* factors were refined using TLS.[14] Because the molecular replacement search model and the final structure were in isomorphous space groups, we inadvertently corrupted the cross-validation test set. To

dx.doi.org/10.1021/bi500594x | *Biochemistry* 2014, 53, 8043−8051

calculate an *a posteriori* R_{free}, we selected a new test set representing 10% of the data.[15] The final model was subjected to simulated annealing using Cartesian molecular dynamics at 2500 K to decouple the test set.[15] The final model statistics are listed in Table 1.

Sedimentation Velocity. Solutions of 0.91 μM hUGDH, 150 mM KCl, and 25 mM buffer [MES (pH 6.5), HEPES (pH 7.5), or Tris (pH 8.5)] were loaded into 12 mm cells and placed in an Optima XLA analytical ultracentrifuge set to 20 °C and 50000 rpm. The $hUGDH_{M11}$ dimer (9.1 μM) was analyzed similarly in 150 mM KCl and 25 mM HEPES (pH 7.5). Sedimentation within the cells was monitored in 0.003 cm step sizes at 230 nm (0.9 μM) or 280 nm (9.0 μM) for 8 h. Raw sedimentation data were modeled using SEDFIT as $c(s)$ distributions that fit baseline and meniscus as well as systematic and time invariant noise.[16] SEDENTERP was used to estimate a partial specific volume of 0.7384 mL g^{-1} and densities of 1.00532, 1.00726, and 1.00603 g mL^{-1} for pH 6.5, 7.5, and 8.5 solutions, respectively.[17] Viscosities for the same pH range were estimated to be 0.01003, 0.010176, and 0.010068 P, respectively.

Steady-State Kinetics and UDP-Xyl Inhibition. Nucleotides NAD^+, NADH, and UDP-Glc were obtained from Sigma. UDP-Xyl was obtained from Carbosource (University of Georgia). All experiments were conducted in a reaction buffer containing 50 mM HEPES or 50 mM Tris, 50 mM NaCl, and 5 mM EDTA. Steady-state kinetic analysis of wild-type hUGDH was conducted using saturating amounts of 2.5 mM NAD^+ with 100 nM hUGDH at pH 7.5 and 230 nM enzyme at pH 8.5. Prior to the reaction, the enzyme and substrates were preincubated separately for 5 min at 25 °C and the reaction was initiated by a rapid manual mixing of the two solutions. An Agilent 8453 UV/vis spectrometer equipped with a Peltier temperature controller was used to follow enzyme reactions by continually monitoring the formation of NADH at 340 nm (molar absorptivity coefficient of 6220 M^{-1} cm^{-1}). All data were analyzed and modeled using nonlinear regression as implemented in PRISM (GraphPad Software Inc., San Diego, CA). Steady-state velocities were calculated by fitting the progress curves to the hysteresis equation derived by Frieden:[10]

$$P(t) = v_{ss}t - \tau(v_{ss} - v_i)(1 - e^{-t/\tau}) \quad (1)$$

where P is the concentration of product at time t and τ is the relaxation time. τ is equal to $1/k_{obs}$, where k_{obs} is the apparent rate constant for the transition between the initial (v_i) and steady-state velocities (v_{ss}) (Figure 1C). It is important to note that v_i in eq 1 is the initial velocity prior to steady state, and only v_{ss} is appropriate for calculating initial steady-state velocities for use in substrate saturation curves (with the caveat that <10% of substrate has been consumed prior to reaching v_{ss}). For steady-state analysis, the substrate saturation curves were fit to a sigmoidal model based on residual analysis:[18]

$$v_o = \frac{k_{cat}[E_t][S]^h}{K_M{}^h + [S]^h} \quad (2)$$

To determine the K_i for the competitive inhibitor UDP-Xyl, steady-state analysis was conducted using different concentrations of UDP-Xyl (see Figure 3 for concentrations). The data from each concentration of UDP-Xyl were simultaneously fit to the equation for competitive inhibition using global analysis in PRISM:

$$v_o = \frac{k_{cat}[E_t][S]^h}{(K_M^{app})^h + [S]^h} \text{ where } K_M^{app} = K_M\left(1 + \frac{[I]}{K_i}\right) \quad (3)$$

Specific activity studies were conducted using saturating amounts of 2.5 mM NAD^+ and 0.3 mM UDP-Glc with 230 nM enzyme at pH 8.4. To determine the pH optimum, reaction mixtures were prepared as separate substrate (2.5 mM NAD^+ and 0.6 mM UDP-Glc) and enzyme (230 nM) solutions in 50 mM buffer (pH 6.0−6.4 for MES, pH 7.0−7.4 for HEPES, pH 7.8−9.0 for Tris, and pH 9.4−10.4 for glycine), 5 mM EDTA, and 50 mM NaCl. Substrate and enzyme solutions were preincubated separately for 5 min at a reaction temperature of 25 °C, and the reaction was initiated by a rapid mixing of the two solutions.

Modeling the Dependence of Specific Activity on Protein Concentration. In our previous work, we showed that the tetramer is a transient in the formation and dissociation of the hexamer.[5,6] In modeling the dependence of hUGDH specific activity on protein concentration, we make the simplifying assumption that the tetramer makes a negligible contribution to specific activity. Thus, our derivation assumes an equilibrium between three low-activity dimers (E_D) and a higher-activity hexamer (E_H):

$$3E_D \overset{K_a}{\leftrightarrow} E_H \quad (4)$$

The hexamer concentration can be expressed as

$$[E_H] = K_a[E_D]^3 \quad (5)$$

The total concentration of enzyme, $[E_T]$, is

$$[E_T] = 2[E_D] + 6[E_H] \quad (6)$$

which can be expressed in terms of the dimer concentration:

$$[E_T] = 2[E_D] + 6K_a[E_D]^3 \quad (7)$$

or

$$0 = 6K_a[E_D]^3 + 2[E_D] - [E_T] \quad (8)$$

Using the general solution for a cubic polynomial, we solve for $[E_D]$ in terms of total enzyme concentration:

$$[E_D] = \sqrt[3]{\frac{[E_T]}{12K_a} + \sqrt{\left(\frac{[E_T]}{12K_a}\right)^2 + \left(\frac{1}{9K_a}\right)^3}} + \sqrt[3]{\frac{[E_T]}{12K_a} - \sqrt{\left(\frac{[E_T]}{12K_a}\right)^2 + \left(\frac{1}{9K_a}\right)^3}} \quad (9)$$

The specific activity (SA) of hUGDH is the sum of the specific activities of the hexamer (SA_H) and dimer (SA_D) multiplied by their molar fraction:

$$SA = \frac{6[E_H]}{[E_T]}SA_H + \frac{2[E_D]}{[E_T]}SA_D \quad (10)$$

Expressing the SA in terms of the dimer concentration (eq 4):

$$SA = \frac{6K_a[E_D]^3}{[E_T]}SA_H + \frac{2[E_D]}{[E_T]}SA_D \quad (11)$$

We can now substitute eq 9 for $[E_D]$ in the expression given above and solve for total specific activity in terms of total

dx.doi.org/10.1021/bi500594x | *Biochemistry* 2014, 53, 8043−8051

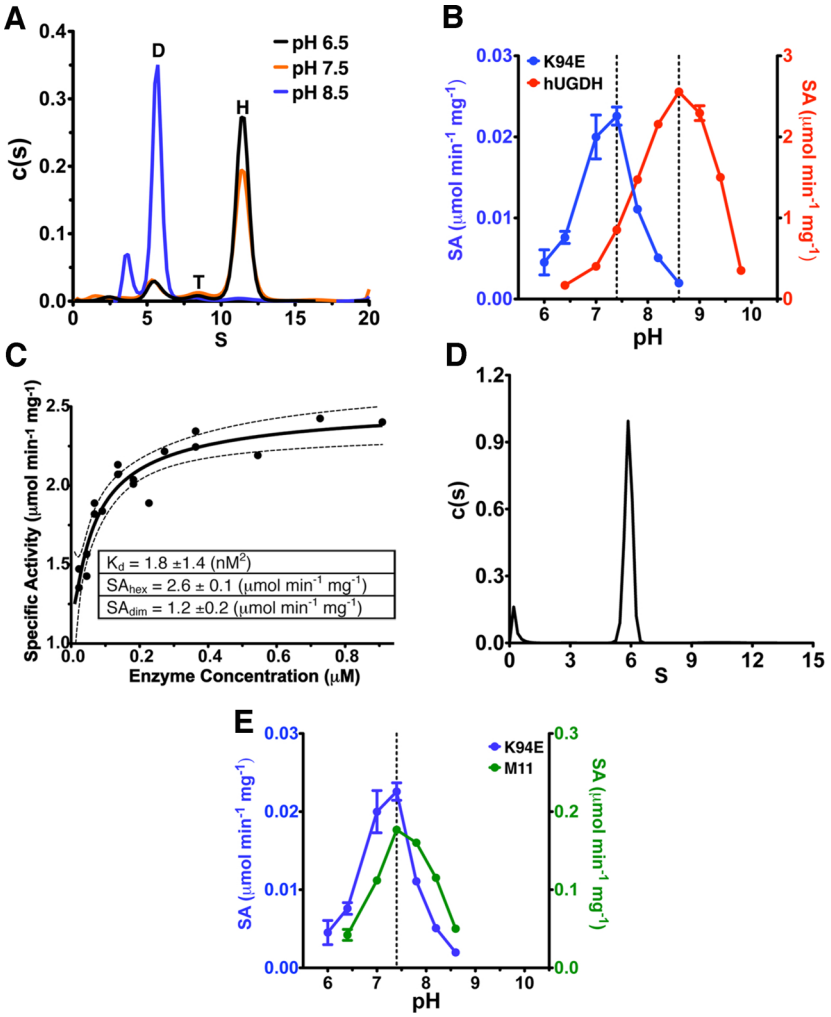

Figure 2. Hexamer stability and activity are pH sensitive. (A) The $c(s)$ sedimentation velocity distributions show that hexameric hUGDH (H, 11.4 S) is stable at pH 6.5−7.5 while the dimer (D, 5.7 S) dominates at pH 8.5. A small amount of tetrameric hUGDH (T, 8.6 S) is also observed. (B) Wild-type hUGDH (red line) and dimeric $hUGDH_{K94E}$ (blue) have pH optima of 8.6 and 7.4, respectively. Specific activities (SAs) are plotted in corresponding colors on opposite Y-axes. (C) The specific activity of hUGDH shows a hyperbolic dependency on enzyme concentration at pH 8.4, consistent with the formation of a more active hexamer. The data were fit (black line) using eq 11. The dotted lines identify the 95% confidence intervals of the fit. The modeled specific activities for the hexamer (SA_{hex}) and dimer (SA_{dim}) are indicated, as well as the dissociation constant $K_d = 1/K_a$ (see the text). (D) The $c(s)$ sedimentation velocity distribution of 9.1 μM $hUGDH_{M11}$ at pH 7.5 reveals a single species at 5.7 S, confirming the dimer structure. (E) Dimeric $hUGDH_{K94E}$ (blue line) and $hUGDH_{M11}$ (green line) have the same pH optima of 7.4, despite different rates. Specific activities (SAs) are plotted in corresponding colors on opposite Y-axes.

enzyme concentration. Specific activity data at different enzyme concentrations were fit using the program PRISM.

RESULTS

The Hexameric Structure of hUGDH Is Destabilized at Alkaline pH. We have previously shown that the apo-hUGDH hexamer dissociates at low protein concentrations.[5] Here, we used analytical ultracentrifugation to study the effects of pH on the oligomeric state. Sedimentation velocity studies of 0.9 μM hUGDH at pH 7.5 show that the $c(s)$ distribution is dominated by an 11.4 S species (77%) corresponding to the hUGDH hexamer. We also observe a 8.6 and 5.4 S species, indicating the presence of a small amount of tetramer (8%) and dimer (15%), respectively (Figure 2A). The hexamer is also favored at pH 6.5 (85% of the distribution), with smaller amounts of tetramer (4%) and dimer (11%) (Figure 2A). In contrast, the hexamer dissociates at alkaline pH. At pH 8.5, 85% of the $c(s)$ distribution is represented by a 5.7 S species consistent with the hUGDH dimer, and the remaining 15% sediments at 3.7 S, indicating a small amount of monomer (Figure 2A). The s-values obtained from rapid equilibrium systems are biased by the mean of the $c(s)$ distribution; thus, the apparent deviation in s-values for the dimer at pH 8.5 and 7.5 (5.7 and 5.4 S, respectively) does not necessarily imply a significant change in the conformation of the protein.[19] These results show that physiological pH stabilizes the hUGDH hexamer.

The Hexameric Structure Alters the Activity of hUGDH. We determined the pH optimum of hUGDH to be ∼8.6, which is consistent with earlier reports (Figure 2B).[2,20] The alkaline pH optimum appears to be at odds with our observation of a dimer at pH 8.5, given that the hexamer is required for maximal catalytic activity (Figure 2A).[6,21] Because cofactor and substrate binding will allosterically induce hexamer formation, it may be that the hexamer is formed under steady-state conditions.[6] To test this possibility, we examined the change in specific activity with respect to enzyme concen-

dx.doi.org/10.1021/bi500594x | Biochemistry 2014, 53, 8043−8051

Table 2. pH Dependence of Hysteresis

pH	v_i (μM/min)[a]	v_{ss} (μM/min)[a]	v_i/v_{ss} (%)	τ (s)[a]	k_{obs} (s^{-1})[b]	lag (s)[c]
6.5	0.047 ± 0.064	7.0 ± 0.05	0.67	70.5 ± 1.8	0.014	191.5 ± 4.8
7.5	2.7 ± 1.7	26.1 ± 0.07	10.3	7.9 ± 0.5	0.127	21.4 ± 1.4
8.5	34 ± 13.3	53.1 ± 1.5	64	3.67 ± 0.22	0.272	9.97 ± 0.6

[a]Data for the progress curves were collected in triplicate except for those at pH 8.5, which are duplicates. Data were fit to eq 1 using global analysis to calculate v_i, v_{ss}, and τ. [b]$k_{obs} = 1/\tau$. [c]Lag was calculated using the equation lag = $e\tau$.

tration. The specific activity of hUGDH displays a hyperbolic dependence on enzyme concentration at pH 8.4 (Figure 2C). The saturable behavior of hUGDH specific activity is consistent with three low-activity dimers (D) undergoing a concentration-dependent association to form a higher-activity hexamer:[6]

$$3[D] \overset{K_a}{\leftrightarrow} [D]^3$$

This model assumes that the tetramer is a negligible species in the association and dissociation of the hexamer and is based on our previous work showing that the tetramer behaves as a transient in the dimer−hexamer equilibrium.[5,6] The change in specific activity due to hexamer formation can be fit to an isotherm relating specific activity to protein self-association using eq 11 (Figure 2C). The fit predicts specific activities of 1.2 ± 0.2 and 2.6 ± 0.1 μmol min^{-1} mg^{-1} for the dimer and hexamer, respectively, and a dissociation constant, K_d, of 1.8 nM^2 for the active hexamer at pH 8.4 (Figure 2C). On the basis of this analysis, the saturating concentration of substrate and cofactor will stabilize the 0.9 μM hUGDH as a hexamer at pH 8.4. In fact, we have previously used sedimentation velocity analysis to show that saturating concentrations of cofactor and substrate will induce hexamer formation at pH 8.0.[6] Thus, the observed pH optimum of 8.6 for hUGDH is associated with the formation of the active hexamer.

Next, we examined the pH optimum of dimeric hUGDH. We have previously described $hUGDH_{K94E}$, a stable dimer of hUGDH that is the result of a charge-switch substitution designed to disrupt the hexamer.[6] $hUGDH_{K94E}$ has a pH optimum of ∼7.4, but the activity (0.023 μmol min^{-1} mg^{-1}) is 37-fold lower than that of the wild-type enzyme at the same pH (0.85 μmol min^{-1} mg^{-1}) (Figure 2B). It has been suggested that the reduced activity in the $hUGDH_{K94E}$ dimer may be due to the destabilization of $loop_{88-110}$, which is involved in cofactor binding.[22] To address this concern, we designed a new, stable dimer construct ($hUGDH_{M11}$) using a triple substitution (F323T/N324T/T325D) in $loop_{323-325}$, which is buried in the hexamer interface. Sedimentation velocity analysis of 9.1 μM $hUGDH_{M11}$ at pH 7.5 reveals a 5.7 S species, consistent with the hUGDH dimer (Figure 2D). This is in contrast to the wild-type enzyme, which forms a stable hexamer at a much lower protein concentration of 0.91 μM (Figure 2A). The activity of $hUGDH_{M11}$ is only 4.7-fold lower than that of the wild-type enzyme hexamer at pH 7.4, which is similar to the 5-fold decrease in activity for the hUGDH dimer reported by others.[22] In addition, both $hUGDH_{M11}$ and $hUGDH_{K94E}$ have the same pH optima of 7.4 (Figure 2E). At pH 8.4, the specific activity of $hUGDH_{M11}$ is ∼22 times lower than what we expected for the wild-type dimer on the basis of our modeling of the specific activity at pH 8.4 (Figure 2B,C,E). It may be that the tetramer is not a negligible species at low protein concentrations in the presence of saturating cofactor and substrate, and that the activity of the tetramer is significant. Thus, the activity that we assigned to the dimer in our model may also include a substantial amount of active tetramer. Still, the goal of the modeling experiment was to determine the protein concentration that stabilizes the hexamer in the presence of saturating substrate and cofactor. In that context, the model predicts 0.9 μM hUGDH will stabilize the hexamer under saturating conditions at pH 8.4, which is consistent with our earlier results from sedimentation velocity analysis.[6]

Hysteresis in hUGDH Is Favored at Physiological pH. Because the E* conformation is an intrinsic property of the hexamer,[7] and the hexamer stability is sensitive to pH, we examined the pH dependency of hUGDH hysteresis. We determined the length of the hysteretic lag, defined as the time taken for the enzyme to reach steady-state velocity. The duration of lag, initial velocity (v_i), and steady-state velocity (v_{ss}) were calculated by fitting progress curves to eq 1 (see Materials and Methods). The lag increases at lower pH, suggesting that the stabilities of E* and the hexamer are correlated (Table 2). We estimated the fraction of active enzyme present when the reaction was initiated (E/E*) by examining the ratio of initial and steady-state velocities obtained from the progress curves (v_i/v_{ss}). If we assume that the E* conformation has no activity (the extreme case), then the v_i/v_{ss} ratio shows that the E* conformation is strongly favored at pH 6.5, with only 0.67% of the enzyme in the E state (Table 2). In contrast, at pH 7.5, 10.3% of the enzyme is present in the active state. When the pH increases to 8.5, 64% of hUGDH is observed to exist in the active, E conformation (Table 2). Even if the E* conformation has a low level of activity, it is clear from this analysis that the E* conformation is favored at lower pH.

hUGDH Is More Sensitive to Inhibition by UDP-Xylose at Physiological pH. At pH 8.5, the substrate saturation curves of hUGDH with respect to UDP-Glc show a small degree of negative cooperativity (Hill coefficient of 0.87 ± 0.08) (Figure 3A and Table 3). In the presence of 20 μM UDP-Xyl, the substrate saturation curves become sigmoidal (Hill coefficient of 1.3 ± 0.08). At the higher concentration of 40 μM UDP-Xyl, the sigmoidicity increases to a Hill coefficient of 1.9 ± 0.07. This type of cooperative behavior in the presence of UDP-Xyl was observed in earlier studies of UGDH.[3,23] UDP-Xyl stabilizes the horseshoe-shaped hexamer, while the cofactor in the presence of substrate stabilizes the active, *32 symmetry* complex (Figure 1A).[6,8] In the horseshoe-shaped hexamer, the Thr131 loop occupies the space that would normally accommodate the C5′-hydroxymethyl of UDP-Glc (Figure 1B).[8] The partially occluded active site would reduce the affinity for UDP-Glc. Thus, the substrate cooperativity we observe in the presence of UDP-Xyl is consistent with the allosteric transition of the horseshoe-shaped complex with low affinity for UDP-Glc into the *32 symmetry* hexamer with higher affinity for the substrate (Figure 1A).

hUGDH is sensitive to product inhibition with a K_i of 27 μM for NADH at pH 7.5.[7] At high protein concentrations, hUGDH can produce inhibitory amounts of NADH before the hysteretic lag ends, thereby complicating steady-state analysis. This can be

dx.doi.org/10.1021/bi500594x | *Biochemistry* 2014, 53, 8043−8051

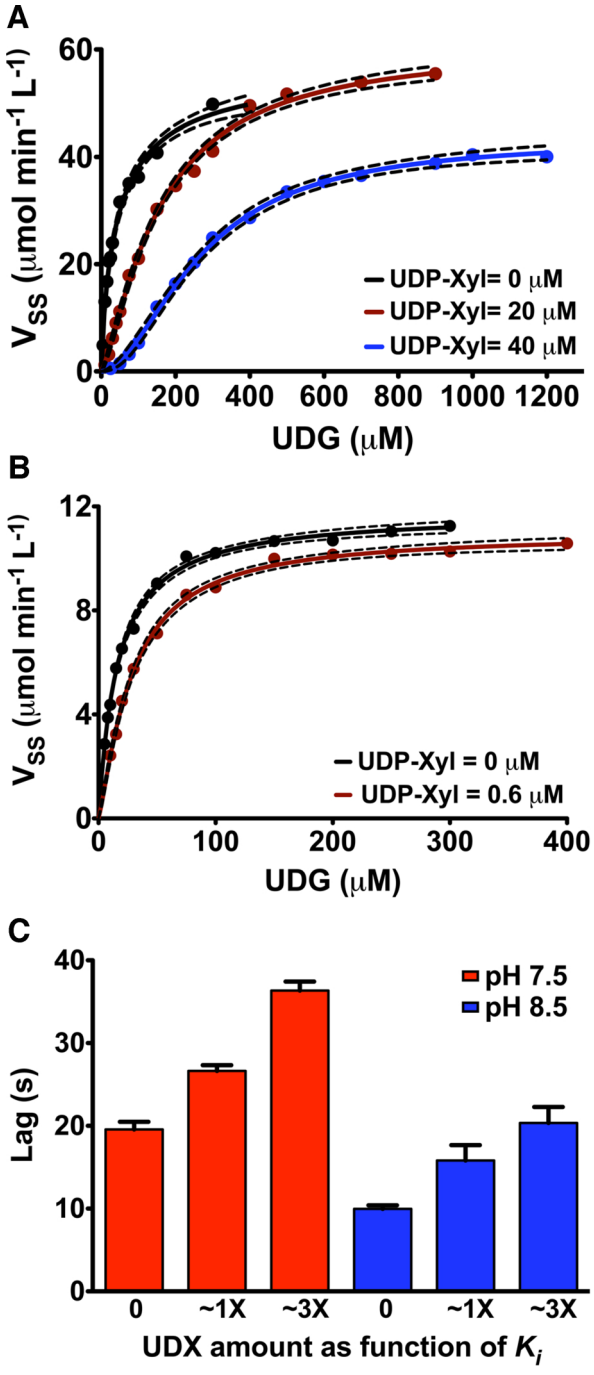

Figure 3. UDP-xylose inhibition is sensitive to pH. (A) At pH 8.5, steady-state analysis of hUGDH in the presence of 0 (black), 20 (red), and 40 μM (blue) UDP-Xyl (UDX) (see Table 3 for parameters). Steady-state velocities were determined with eq 1. Because of the increased lag and resulting product inhibition with 40 μM UDP-Xyl, only the 0 and 20 μM UDX data were globally fit to the equation for competitive inhibition, modified for cooperativity (see the text and Materials and Methods). Dotted lines indicate 95% confidence intervals. (B) Same as above, but at pH 7.5 with UDP-Xyl at 0 (black) and 0.6 μM (red). (C) The hUGDH hysteretic lag increases with UDP-Xyl concentration at pH 7.5 (red) and 8.5 (blue). UDP-Xyl concentrations are reported in units of K_i (0.81 and 6.98 μM for pH 7.5 and 8.5, respectively).

avoided by keeping protein concentrations low and measuring the amount of NADH produced before reaching steady-state velocity, as we have previously described.[7] Here, our data show that UDP-Xyl inhibition increases the lag (Figure 3C). Conditions that increase the length of the lag at a constant protein concentration could produce inhibitory concentrations of NADH before reaching the steady state. In fact, at 40 μM UDP-Xyl (~6K_i), >18 μM NADH is produced before the lag ends (data not shown). This explains the apparent decrease in k_{cat} for the substrate saturation curve at 40 μM UDP-Xyl (Figure 3A and Table 3). Therefore, we excluded the 40 μM UDP-Xyl data from our determination of the K_i for UDP-Xyl. Because UDP-Glc and the allosteric inhibitor compete for the active site, we fit the 0 and 20 μM UDP-Xyl data to a cooperative model for competitive inhibition using global analysis (eq 3 in Materials and Methods and Table 3). This analysis shows that the K_i for UDP-Xyl at pH 8.5 is 6.98 ± 1.6 μM. Next, we examined UDP-Xyl inhibition at pH 7.5. To prevent product inhibition from occurring during the lag at pH 7.5, we reduced the protein concentration to 100 nM. The substrate saturation curve at pH 7.5 is hyperbolic with respect to UDP-Glc (Figure 3A and Table 3). However, in the presence of 0.6 μM UDP-Xyl, the saturation curves begin to display substrate cooperativity, with a Hill coefficient of 1.24 ± 0.06. The K_i for UDP-Xyl at pH 7.5 is 0.81 ± 0.12 μM, representing a 8.6-fold higher affinity for UDP-Xyl at physiological pH (Figure 3B and Table 3).

Crystal Structure of the E* Complex. Our data show that physiological pH promotes hUGDH hysteresis, favors UDP-Xyl inhibition, and stabilizes the hexamer. To crystallize the E* complex of hUGDH, we targeted the narrow pH range of 6.0–7.5 using nonionic precipitants for crystallization. Crystals were obtained at pH 7.0 and diffracted to a resolution of 2.7 Å. On the basis of our hysteresis data, >90% of hUGDH should be in the E* conformation at pH 7.0 (Table 2). The crystal structure contains three chains in the asymmetric unit corresponding to the top half of a complete hexamer (Figure 4A). The complete hexamer is formed by the operation of a crystallographic 2-fold axis. Residues 383–388 in chains A and B, residues 383–387 in chain C, and the C-terminal tail (residues 467–494) in all three chains in the asymmetric unit are disordered.

The NAD^+ and nucleotide sugar binding domains of hUGDH are flexible and can rotate from a closed to an open conformation in a concerted motion without disrupting the hexamer (Figure 4B).[5] The open form allows the Thr131 loop to change conformation and repack in response to UDP-Xyl binding.[5] The domains of the E* crystal structure are in the "open" conformation. DynDom analysis shows that the NAD^+ binding domains have rotated open by 10.3° relative to the closed conformation of hUGDH (PDB entry 2Q3E).[24] The hinge bending axis is between residues 219 and 222 and has been described in detail elsewhere.[4,5] The structure of E* is most similar to that of the $hUGDH_{\Delta 132}$ construct (PDB entry 3TF5); 2730 corresponding C_α atoms of the E* and $hUGDH_{\Delta 132}$ hexamers superimpose with a 0.9 Å root-mean-square deviation. With the exception of the mutation in $hUGDH_{\Delta 132}$, a minor difference in domain conformation is the only variation between the structures; the domains of the E* structure are 2° less open than those in the $hUGDH_{\Delta 132}$ crystal structure. The strong similarities between the E* and $hUGDH_{\Delta 132}$ hexamers are intriguing, given that the $hUGDH_{\Delta 132}$ construct was designed to trap the allosteric Thr131 loop–α6 switch in an intermediate conformation between the active and inactive states.[5] In fact, the most significant observation in the E* structure involves the Thr131 loop–α6 allosteric switch, which does adopt an intermediate

dx.doi.org/10.1021/bi500594x | *Biochemistry* 2014, 53, 8043–8051

Table 3. Global Fit of Data from UDP-Xylose Inhibition Studies

pH	[UDP-Xyl] (μM)	[hUGDH] (μM)	UDP-Glc K_M (μM)[a]	k_{cat} (s^{-1})[a]	UDP-Xyl K_i (μM)[a]	Hill coefficient (h)[a]
8.5	0	0.23	43.4 ± 6.7	4.17	6.98 ± 1.6	0.87 ± 0.08
	20			4.62		1.3 ± 0.08
	40[b]			3.12		1.9 ± 0.07
7.5	0	0.10	16.1 ± 0.79	1.97	0.81 ± 0.12	1.02 ± 0.05
	0.6			1.83		1.24 ± 0.06

[a]The kinetic parameters, K_M, K_i, k_{cat}, and h, were calculated using a global analysis of the inhibition data using eqs 2 and 3. [b]The 40 μM UDP-Xyl sample was not used in calculating K_i because of significant product inhibition (see the text).

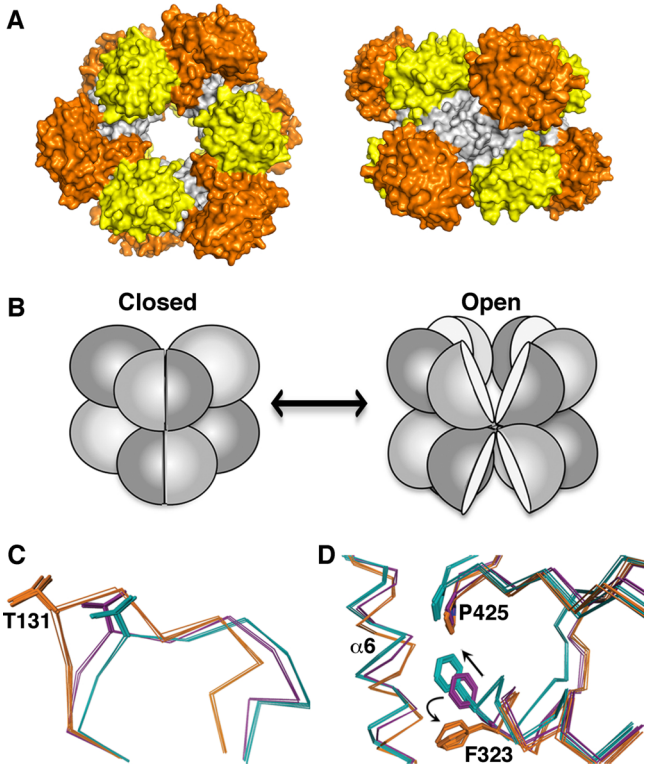

Figure 4. Crystal structure of the E* complex. (A) Top and side views of the E* hexamer. The NAD^+ (orange), nucleotide sugar binding domain (yellow) and dimerization domain (gray) are depicted. (B) Cartoon showing the closed and open conformations of the NAD^+ and nucleotide sugar binding domains. (C) Superposition of the Thr131 loop of the E* (magenta), active *32 symmetry* hexamer (cyan, PDB entry 2Q3E) and the horseshoe-shaped hexamer (orange, PDB entry 3PTZ). To illustrate the small degree of variability in the position of the Thr131 loop, all of the unique chains contained in the asymmetric unit of each crystal structure are superimposed. (D) Hexamer building interface illustrated as in panel C. The α6 helix (α6), $loop_{322-324}$ (F323), and Pro425 (P425) are shown. Black arrows depict the motions that Phe323 undergoes to switch states.

conformation (Figure 4C). In our earlier work, we showed that the hUGDH domains can close only if the Thr131 loop is in the active or inactive state.[5] The intermediate E* conformation traps the domains in the "open" state; closure of the domains would result in steric clashes similar to what we observe in the $hUGDH_{\Delta 132}$ structure.[5]

The Thr131 loop in the E* structure is shifted 0.9 Å from the active conformation and toward the inactive state (Figure 4C). In this position, the substrate and cofactor binding sites are partially occluded. The position of the C_α atom of Thr131 varies by only 0.1 Å among the three unique molecules in the asymmetric unit. The interface between adjacent dimers of the E* hexamer also adopts a conformation between the active and inactive states (Figure 4D). To form the inactive state, the feedback inhibitor UDP-Xyl induces the α6 switch helix to translate ~1.43 Å and rotate 10.3°, and the χ_1 torsion angle of Ser139 rotates 158° (Figure 4D).[8] A compensatory repacking of Pro425 and $loop_{322-324}$ in the adjacent dimer accommodates the shift of the α6 switch helix. Most notably, the C_α atom of Phe323 translates 2.0 Å and the χ_1 torsion angle rotates −60.6°. The interface in the E* structure is in an intermediate conformation in the transition from the active to the horseshoe hexamers. (i) The α6 switch helix has translated ~0.7 Å and rotated by 9.0°. (ii) The χ_1 torsion angle of Ser139 rotated by 114.0°. (iii) The χ_1 torsion angle of Phe323 has rotated −8.6°, and the C_α atom has shifted 1.6 Å. On the basis of these observations, we believe that the role of the E* structure is to facilitate feedback inhibition by shifting the conformation of the hUGDH subunits toward the inactive state.

DISCUSSION

The formation of the hUGDH hexamer is under allosteric control.[5,6,8] Cofactor binding enhances the affinity among three weakly interacting dimers to induce formation of a stable 32 *symmetry* hexamer (Figure 1A,B).[6] Similarly, the feedback inhibitor UDP-Xyl induces formation of a stable but inactive horseshoe-shaped hexamer.[8] Earlier work showed that hysteresis in hUGDH is not due to hUGDH dimers associating to form a more active hexamer; instead, a cofactor and substrate induced isomerization of hUGDH from a less active E* to a more active E conformation (Figure 1D).[7] Here, we have investigated the role of the E* state in enzyme activity and feedback inhibition. First we show that the E* state is favored at physiological pH. The length of the hysteretic lag in progress curves increases as the pH decreases from 8.5 to 6.5, suggesting that E* is favored at the lower pH. Analysis of the v_i/v_{ss} ratio of the lag also predicts a larger fraction of E*/E at the lower pHs assuming E* is inactive (Table 2). However, even if E* has a low level of activity, the E*/E ratio is consistent with the stabilization of E* at lower pH values. Finally, sedimentation velocity studies show that the hexamer is stabilized at lower pH values (Figures 1C and 2A). This is important because the E* conformation is an intrinsic property of the hexamer (Figure 1C).[7]

Next, we determined the crystal structure of hUGDH under conditions that stabilize the E* complex. The v_i/v_{ss} ratio suggests that between 90 and 99.3% of hUGDH is in the E* conformation between pH 7.5 and 6.5 (Table 2). Thus, the stable hexamer observed at physiological pH in sedimentation velocity studies most likely represents the E* conformation (Figure 2A). This is also good evidence that the crystal structure at pH 7.0 represents the authentic E* conformation (Figure 4). The crystal structure of E* closely resembles the $hUGDH_{\Delta 132}$ construct (PDB entry 3TF5), which was designed

dx.doi.org/10.1021/bi500594x | *Biochemistry* 2014, 53, 8043−8051

to mimic an intermediate in the allosteric transition between the active and inactive states.[5] In fact, at physiological pH, the Thr131 loop−α6 switch in hUGDH adopts a conformation that appears to be an intermediate in the transition from the active *32 symmetry* hexamer to the inactive, horseshoe-shaped complex (Figure 4C,D). To accommodate this conformation, the domains of hUGDH have rotated to the open conformation (Figure 4B). The open domain conformation is essential for the Thr131 loop−α6 switch to change conformations.[5] One result of this intermediate conformation is that the active site is partially occluded, meaning that the Thr131 loop−α6 switch will have to move to bind cofactor and substrate (Figure 4C,D). We believe that this intermediate conformation represents E* and that the transient observed in progress curves is due to the isomerization of the Thr131 loop−α6 allosteric switch and closing of the domains to adopt the active conformation. But what is the function of the E* conformation in hUGDH? We believe that the E* conformation facilitates feedback inhibition by shifting the Thr131 loop−α6 switch helix into a conformation closer to the inhibited state. In fact, hUGDH is 8.6-fold more sensitive to UDP-Xyl inhibition at pH 7.5 than at pH 8.5 (Figure 3 and Table 3). Previous studies have reported a similar pH dependence of the UDP-Xyl K_i.[23,25] It is likely that the hexamer restrains the enzyme in the E* conformation at physiological pH. In fact, the data show that the formation of the hexamer alters the activity of the enzyme. The pH optimum of the hUGDH hexamer is 8.6, but that of the dimer is 7.4 (Figure 2B,E). The fact that the hexamer and dimer have the same active sites suggests that formation of the hexamer favors an enzyme conformation with an alkaline pH optimum. We also note that the alkaline pH shift in catalytic activity is correlated with a weaker hexameric complex (Figure 2A). Thus, it would appear that the stable hexamer at physiological pH restrains the structure in the E* conformation.

The observation of a stable, E* conformation also explains accounts of substrate cooperativity only in the presence of UDP-Xyl (Figure 3 and Table 3).[3,23] The sigmoidicity is consistent with a cooperative transition from the inactive, horseshoe-shaped complex to the active, *32 symmetry* hexamer, assuming the former structure has a lower affinity for UDP-Glc. In fact, the conformation of the Thr131 loop−α6 allosteric switch in the active site of the horseshoe-shaped hexamer is specific for UDP-Xyl and introduces a steric clash with the C6′-hydroxyl of UDP-Glc.[8] As UDP-Glc outcompetes UDP-Xyl, the conformation of hUGDH would switch to the *32 symmetry* hexamer, which would have a higher affinity for UDP-Glc, thus explaining the substrate cooperativity observed in the presence of UDP-Xyl. But if hUGDH is a cooperative enzyme, why are the saturation curves for UDP-Glc hyperbolic in the absence of UDP-Xyl? Studies have shown that allosteric enzymes whose active and inactive states bind substrate with equal affinity will have hyperbolic substrate saturation curves.[26] However, if a competitive inhibitor shows a distinct preference for binding to the inactive state, the substrate saturation curves will become sigmoidal in the presence of the inhibitor (Figure 3 and Table 3).[26] Thus, if the active and E* conformations of hUGDH both display equal affinity for UDP-Glc, the substrate saturation curves will be hyperbolic. The cooperativity will be observed only after UDP-Xyl triggers the formation of the horseshoe complex with a reduced affinity for UDP-Glc (Figures 1B and 3). Similar behavior has been observed in anabolic ornithine transcarbamoylase and L-alanine dehydrogenase, which show cooperativity in substrate saturation curves only in the presence of a competitive inhibitor that favors the inactive conformation of the enzyme.[26−28]

Finally, we turn our attention to the formation of the inactive horseshoe hexamer (Figure 1A). Specifically, what is the source of the initial asymmetry that causes the *32 symmetry* hexamer to dissociate preferentially along one interface to form the horseshoe complex? We believe that substoichiometric binding of UDP-Xyl triggers the asymmetry that produces the horseshoe hexamer (Figure 5). As UDP-Xyl binds to a specific

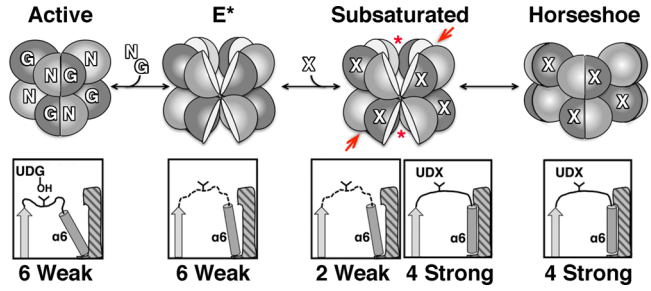

Figure 5. Model for the activation and UDP-Xyl inhibition of the E* hexamer. The hexamer is depicted in the active, E*, subsaturated, and horseshoe states. The insets below each state illustrate the conformation of Thr131 loop−α6 switch as a loop connecting a gray strand to the α6 helix (gray cylinder). The hexamer interface is shown as a hatched surface complementary to the α6 helix. The loop is depicted in ligand-bound (—) and intermediate (---) conformations. Thr131 (the "Y" structure in the loop) interacts with UDP-Glc (UDG) or UDP-Xyl (UDX). The strong and weak interfaces are identified. The binding of NAD^+ (N) and UDP-Glc (G) to E* generates the closed, active structure with a weak, flexible hexamer interface.[5] The binding of substoichiometric amounts of UDP-Xyl (X) produces a subsaturated complex with a mix of strong and weak interfaces. The UDP-Xyl-bound subunits rotate the α6 helix to create a strong interface. The red asterisk indicates the weaker interface between the two unbound subunits (red arrow). Dissociation along the weak interface will allow the subunits to undergo a rigid body rotation to close the domains without disrupting the UDP-Xyl-stabilized interfaces.

subunit in E*, the Thr131 loop−α6 switch can be switched to the inactive state while the domains remain open. In fact, our earlier work showed that the interface between adjacent dimers in the domain "open" hexamer can adopt the horseshoe conformation without disrupting the *32 symmetry*.[5] We have also shown that the interface of the UDP-Xyl-induced hexamer is more stable than the UDP-Glc interface.[5,8] Thus, substoichiometric binding of UDP-Xyl can result in an "open" domain hexamer with a mix of strong and weak interfaces (Figure 5). The domains in such a hexamer can close in one of two ways. (i) To maintain *32 symmetry*, the domains must disrupt the stable contacts in the UDP-Xyl-buttressed interfaces to rotate to the "closed" state, or (ii) to form the horseshoe hexamer, the weaker UDP-Xyl-free interface can dissociate to allow the dimers to rotate as rigid bodies and close the domains without disrupting the two remaining interfaces.

On the basis of the results we have presented here, we propose that at physiological pH, the hexameric structure of hUGDH restrains the enzyme in a less active conformation that favors feedback inhibition by UDP-Xyl. This conformational leveraging allows the small difference in the effector molecule (the absence of a C5′-hydroxymethyl) to induce a disproportionately larger allosteric transition. This "conformational leveraging" by the formation of a higher-order quaternary

dx.doi.org/10.1021/bi500594x | *Biochemistry* 2014, 53, 8043−8051

structure is not without precedent. A similar behavior is observed in mammalian hemoglobin. The individual $\alpha\beta$ hemoglobin dimers have a high affinity for oxygen.[29] However, formation of the $(\alpha\beta)_2$ tetramer restrains the subunits to a lower-affinity conformation, which is essential for oxygen delivery.

■ ASSOCIATED CONTENT

Accession Codes

The atomic coordinates and structure factors have been deposited in the Protein Data Bank as entry 4RJT.

■ AUTHOR INFORMATION

Corresponding Author

*E-mail: zac@bmb.uga.edu. Phone: (706) 583-0304. Fax: (706) 542-1738.

Author Contributions

†R.K. and G.S.C. contributed equally to this work.

Funding

Funding from the University of Georgia Research Alliance and American Cancer Society Grant RSG0918401DMC to Z.A.W. is gratefully acknowledged.

Notes

The authors declare no competing financial interest.

■ ABBREVIATIONS

hUGDH, human UDP-α-D-glucose-6-dehydrogenase; PDB, Protein Data Bank; UDG, UDP-α-D-glucose; UDX, UDP-α-D-xylose.

■ REFERENCES

(1) Kalckar, H. M., Maxwell, E. S., and Strominger, J. L. (1956) Some properties of uridine diphosphoglucose dehydrogenase. *Arch. Biochem. Biophys. 65*, 2−10.

(2) Gainey, P. A., and Phelps, C. F. (1972) Uridine diphosphate glucuronic acid production and utilization in various tissues actively synthesizing glycosaminoglycans. *Biochem. J. 128*, 215−227.

(3) Balduini, C., Brovelli, A., De Luca, G., Galligani, L., and Castellani, A. A. (1973) Uridine diphosphate glucose dehydrogenase from cornea and epiphysial-plate cartilage. *Biochem. J. 133*, 243−249.

(4) Egger, S., Chaikuad, A., Kavanagh, K. L., Oppermann, U., and Nidetzky, B. (2010) UDP-glucose dehydrogenase: Structure and function of a potential drug target. *Biochem. Soc. Trans. 38*, 1378−1385.

(5) Sennett, N. C., Kadirvelraj, R., and Wood, Z. A. (2011) Conformational Flexibility in the Allosteric Regulation of Human UDP-α-D-Glucose 6-Dehydrogenase. *Biochemistry 50*, 9651−9663.

(6) Sennett, N. C., Kadirvelraj, R., and Wood, Z. A. (2012) Cofactor Binding Triggers a Molecular Switch To Allosterically Activate Human UDP-α-D-glucose 6-Dehydrogenase. *Biochemistry 51*, 9364−9374.

(7) Kadirvelraj, R., Sennett, N. C., Custer, G. S., Phillips, R. S., and Wood, Z. A. (2013) Hysteresis and negative cooperativity in human UDP-glucose dehydrogenase. *Biochemistry 52*, 1456−1465.

(8) Kadirvelraj, R., Sennett, N. C., Polizzi, S. J., Weitzel, S., and Wood, Z. A. (2011) Role of Packing Defects in the Evolution of Allostery and Induced Fit in Human UDP-Glucose Dehydrogenase. *Biochemistry 50*, 5780−5789.

(9) Dickinson, F. M. (1988) Studies on the unusual behaviour of bovine liver UDP-glucose dehydrogenase in assays at acid and neutral pH and on the presence of tightly bound nucleotide material in purified preparations of this enzyme. *Biochem. J. 255*, 775−780.

(10) Frieden, C. (1970) Kinetic aspects of regulation of metabolic processes. The hysteretic enzyme concept. *J. Biol. Chem. 245*, 5788−5799.

(11) Kabsch, W. (2010) Xds. *Acta Crystallogr. D66*, 125−132.

(12) Adams, P. D., Afonine, P. V., Bunkoczi, G., Chen, V. B., Davis, I. W., Echols, N., Headd, J. J., Hung, L. W., Kapral, G. J., Grosse-Kunstleve, R. W., McCoy, A. J., Moriarty, N. W., Oeffner, R., Read, R. J., Richardson, D. C., Richardson, J. S., Terwilliger, T. C., and Zwart, P. H. (2010) PHENIX: A comprehensive Python-based system for macromolecular structure solution. *Acta Crystallogr. D66*, 213−221.

(13) Emsley, P., Lohkamp, B., Scott, W. G., and Cowtan, K. (2010) Features and development of Coot. *Acta Crystallogr. D66*, 486−501.

(14) Urzhumtsev, A., Afonine, P. V., and Adams, P. D. (2013) TLS from fundamentals to practice. *Crystallogr. Rev. 19*, 230−270.

(15) Brunger, A. T. (1997) Free R Value: Cross-validation in Crystallography. *Methods Enzymol. 277*, 366−396.

(16) Schuck, P. (2000) Size-distribution analysis of macromolecules by sedimentation velocity ultracentrifugation and Lamm equation modeling. *Biophys. J. 78*, 1606−1619.

(17) Laue, T. M., Shah, B. D., Ridgeway, T. M., and Pelletier, S. L. (1992) Computer-aided interpretation of analytical sedimentation data for proteins. In *Analytical ultracentrifugation in biochemistry and polymer science* (Harding, S. E., Rowe, A. J., and Horton, J. C., Eds.) pp 90−125, The Royal Society of Chemistry, Cambridge, U.K.

(18) Cornish-Bowden, A. (2001) Detection of errors of interpretation in experiments in enzyme kinetics. *Methods 24*, 181−190.

(19) Schuck, P. (2003) On the analysis of protein self-association by sedimentation velocity analytical ultracentrifugation. *Anal. Biochem. 320*, 104−124.

(20) Gainey, P. A., Pestell, T. C., and Phelps, C. F. (1972) A study of the subunit structure and the thiol reactivity of bovine liver uridine diphosphate glucose dehydrogenase. *Biochem. J. 129*, 821−830.

(21) Hyde, A. S., Farmer, E. L., Easley, K. E., van Lammeren, K., Christoffels, V. M., Barycki, J. J., Bakkers, J., and Simpson, M. A. (2012) UDP-glucose dehydrogenase polymorphisms from patients with congenital heart valve defects disrupt enzyme stability and quaternary assembly. *J. Biol. Chem. 287*, 32708−32716.

(22) Hyde, A. S., Thelen, A. M., Barycki, J. J., and Simpson, M. A. (2013) UDP-glucose dehydrogenase activity and optimal downstream cellular function require dynamic reorganization at the dimer-dimer subunit interfaces. *J. Biol. Chem. 288*, 35049−35057.

(23) Gainey, P. A., and Phelps, C. F. (1975) Interactions of urdine diphosphate glucose dehydrogenase with the inhibitor urdine diphosphate xylose. *Biochem. J. 145*, 129−134.

(24) Hayward, S., and Berendsen, H. J. (1998) Systematic analysis of domain motions in proteins from conformational change: New results on citrate synthase and T4 lysozyme. *Proteins 30*, 144−154.

(25) Huang, Y. H., Roy-Burman, P., and Visser, D. W. (1971) Uridine diphosphate glucose dehydrogenase of calf liver. Properties and inhibition characteristics with uridine diphosphate xylose analogues. *Biochem. Pharmacol. 20*, 2447−2458.

(26) Kuo, L. C. (1983) Allosteric cofactor-mediated enzyme cooperativity: A theoretical treatment. *Proc. Natl. Acad. Sci. U.S.A. 80*, 5243−5247.

(27) Kuo, L. C., Lipscomb, W. N., and Kantrowitz, E. R. (1982) Zn(II)-induced cooperativity of *Escherichia coli* ornithine trans-carbamoylase. *Proc. Natl. Acad. Sci. U.S.A. 79*, 2250−2254.

(28) Kim, S. J., Kim, Y. J., Seo, M. R., and Jhun, B. S. (2000) Regulatory mechanism of L-alanine dehydrogenase from *Bacillus subtilis*. *Bull. Korean Chem. Soc. 21*, 1217−1221.

(29) Hewitt, J. A., Kilmartin, J. V., Eyck, L. F., and Perutz, M. F. (1972) Noncooperativity of the dimer in the reaction of hemoglobin with oxygen (human-dissociation-equilibrium-sulfhydryl-absorption-X-ray analysis). *Proc. Natl. Acad. Sci. U.S.A. 69*, 203−207.

(30) Diederichs, K., and Karplus, P. A. (1997) Improved R-factors for diffraction data analysis in macromolecular crystallography. *Nat. Struct. Biol. 4*, 269−275 592 (Erratum).

(31) Karplus, P. A., and Diederichs, K. (2012) Linking crystallographic model and data quality. *Science 336*, 1030−1033.

(32) Chen, V. B., Arendall, W. B., III, Headd, J. J., Keedy, D. A., Immormino, R. M., Kapral, G. J., Murray, L. W., Richardson, J. S., and Richardson, D. C. (2010) MolProbity: All-atom structure validation for macromolecular crystallography. *Acta Crystallogr. D66*, 12−21.